



# A Force-Sensitive Mechanical Deep Rolling Tool for Process Monitoring

J. Berlin<sup>1</sup>(✉), B. Denkena<sup>1</sup>, H. Klemme<sup>1</sup>, O. Maiss<sup>2</sup>, and M. Dowe<sup>3</sup>

<sup>1</sup> Institute of Production Engineering and Machine Tools (IFW), An der Universität 2, 30823 Garbsen, Germany

berlin@ifw.uni-hannover.de

<sup>2</sup> ECOROLL AG, Celle, Germany

<sup>3</sup> MCU GmbH & Co. KG, Maierhöfen, Germany

**Abstract.** Deep rolling is an efficient process to increase the service life of highly stressed components such as crankshafts or roller bearings by inducing compressive residual stresses. The residual stresses correspond to the deep rolling force applied. Monitoring the deep rolling force enables the processing result to be assessed. The rolling force is a two-dimensional vector. However, current approaches only allow the measurement of one dimension. Thus, this article presents a force-sensitive deep rolling tool that can measure the applied deep rolling force in two axes. This article, describes the principle of the sensory deep rolling tool and its calibration process. Finally, the sensory properties are evaluated.

**Keywords:** Mechanical deep rolling · Surface modification · Sensors

## 1 Introduction

In aerospace or automotive industries, cyclic loads are often the limiting factor for the service life of components, since they lead to fatigue failures [1, 6]. Material fatigue causes more than 80% of all failures occurring during service [4]. Thus, increasing the fatigue strength of the workpiece is important. Surface treatments are an efficient way to achieve this. Surface treatments can be classified in thermochemical, thermal and mechanical treatments [3]. Most commonly used processes for mechanical surface treatment are shot peening, laser shock peening and deep rolling [2]. The advantages of deep rolling are a simple integration in production lines, a high process speed, cost-effectiveness and a large effective processing depth [5, 7]. Deep rolling tools (DRT) use balls or rollers that are pressed against the surface of the workpiece to plastically deform it. Thereby, three positive effects improving fatigue life are achieved. First, the roughness of the surface is reduced, minimizing the notch effect. Secondly, strain hardening is caused by the plastic deformation of the surface, and thirdly, the induction of compressive residual stresses reduces the tensile stresses under cyclic loads [3]. The combination of these effects reduces the crack growth, which usually leads to fatigue failure [6, 7]. Nevertheless, to achieve the desired effect, the rolling force need to be set properly [7, 9]. The force can be applied hydraulically or mechanically [1]. Mechanical

deep rolling has the advantage that no hydraulic unit is needed. In mechanical deep rolling, the deep rolling force results from the deflection of a spring that is integrated in the DRT. A changing deflection thus results in a changing force [8]. Geometric errors of the workpiece cause a changing force, as shown in Fig. 1. To reduce this effect, a high compliance of the spring is desirable. Nevertheless, a force error always remains.

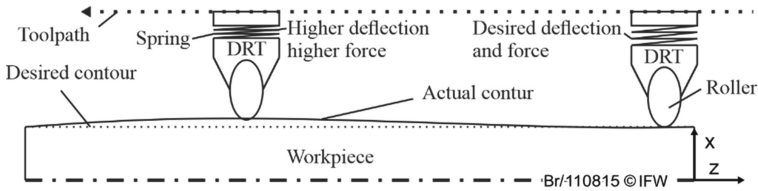


**Fig. 1.** Basics of mechanical deep rolling

The ability to monitor the rolling force during mechanical deep rolling enables a detection of the force errors and is consequently a requirement for process monitoring. To measure the two-dimensional force vector, a force-sensitive DRT is needed. To equip the DRT with force-sensitive properties, strain gauges (SG) can be used. Using SG is a common way to implement force measurement capabilities into tools or machine components. E.g., in the past, axis-slides [10], spindles [11], cutting tools [14] or clamping systems [12] were fitted with SG. However, there is only one approach known from the state of the art dealing with SG implementation into a DRT. This tool determines one dimension of the rolling force vector by measuring the deflection of the spring that is integrated in the tool [13]. However, SG do not measure the forces directly, but only measure the resulting strain on the material surface. The force is calculated based on the strain using a transfer matrix ( $M$ ). That matrix transfers the strain signal vector into a force vector. However, machine tools have a high stiffness. Accordingly, the measurable strain is low. Usually, the main challenge is to achieve sufficient strain and a high force-sensitivity, but to avoid a decrease in the tool's stiffness [10–12]. Mechanical DRT, however, need to be compliant to compensate for geometric errors of the workpiece. For the design of a force-sensitive DRT, this means that the stiffness of the DRT components can be reduced to achieve higher strains and thus a higher force sensitivity. The adequate placement of the SG is another challenge as the location of the SG affects the multi-axis force measurement capability. The matrix  $M$  can be used to evaluate the placement of the SG by analyzing the column vectors of  $M$ . Column vectors that are perpendicular to one another indicate that the matrix  $M$  is well conditioned and the placement of the SG is thus favorable [12].

In the first chapter of this work a mechanical model of a DRT for multi-axis force measurement is presented. The mechanical model is then turned into a rough design based on an existing DRT. The rough design is optimized using a simulation and the placement of the SG is evaluated. For the evaluation, the matrix  $M$  is examined. On the basis of the simulation results the tool was realized. Finally, the tool was calibrated and evaluated based on measurements.

## 2 Implementation of the Sensory Capabilities

The minor stiffness requirements of the DRT allow an unusual approach to measure the force with SG. In order to achieve a high sensitivity, a flexible tool holder was designed. This is intended to achieve nominal strains of  $1000 \mu\text{m/m}$ . A high level of sensitivity is therefore to be expected. Figure 2 illustrates a mechanical model of a DRT with a flexible tool holder. The model consists of two perpendicularly aligned bending beams for each direction of force. One SG is attached to each beam to measure the strain. By decoupling the bending beams with the help of a floating joint and a flexure joint, only one beam is deformed significantly for each load direction. Under the load of  $F_{x'}$ , the force is transmitted through the tool body to the bending beam  $x'$ . The floating joint ensures that the bending beam  $y'$  is loaded with minimal force. Under the load of  $F_{y'}$ , the bending beam  $y'$  is subjected to bending. The bending beam  $x'$ , on the other hand, only experiences a low tensile load, which leads to significantly lower strains. This distribution of the load is intended to ensure that each SG is sensitive for one direction of force and thereby an adequate differentiation between the directions of force is achieved.

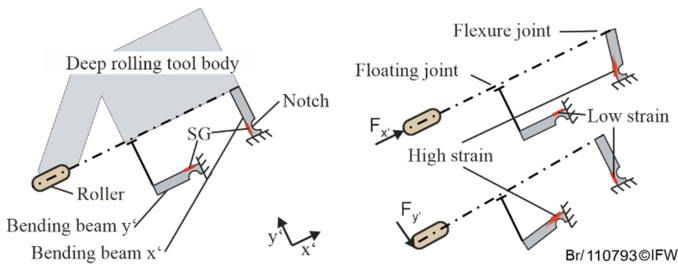


**Fig. 2.** Mechanical model of the deep rolling tool

In a next step the mechanical model was transferred to a rough design of the DRT. A DRT ECOROLL EG45 was used as a basis for the sensory DRT. The EG45 is designed for a maximum load of 4 kN. The adopted components of EG45 provide a spring travel of 2 mm. The bending beams were integrated into the tool holder of EG45 according to Fig. 3. A thin beam with a thickness of 3 mm was used as a floating joint. The beam can transmit tensile and compressive forces, but offers little resistance to forces transverse to it. The flexure joint was realized by a deep notch in the bending beam  $x'$ . Shear forces as well as tensile and compressive forces can still be transmitted. However, the flexure joint is compliant to bending moments. Placing the SGs in the space between the beams ensures protection from external influences like chips, coolant or mechanical damage. Prefabricated SG full Wheatstone bridges (ME type N2A-06) were used. Two electrical resistors of the measuring bridge are aligned to the direction of strain and two are aligned vertically. As a result, the sensitivity is equal to a half-bridge. However, the two additional resistors compensate temperature influences.

A simulation in ANSYS was used to optimize the dimensions of the rough design in Fig. 3. For the simulation model, the tool body was geometrically simplified. The maximum nominal force of 4 kN was applied to the model in  $x'$  and  $y'$  directions and the

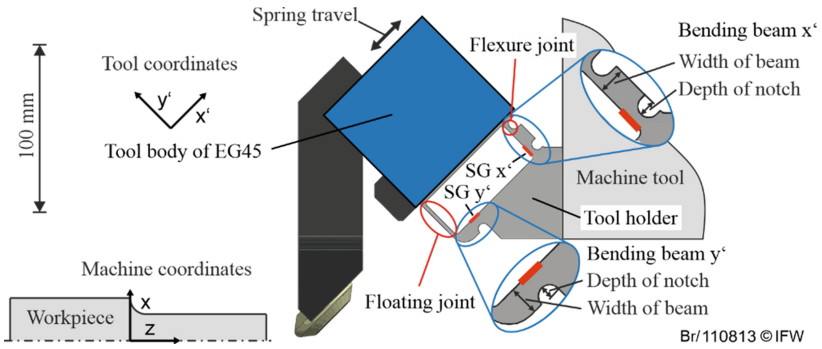


**Fig. 3.** Rough design of the deep rolling tool

resulting strains were analyzed. In a parameter study, the width of the bending beams and the depth of the notches were varied in order to achieve a maximum nominal strain of  $1000 \mu\text{m/m}$  at the positions of the SG. A width of  $8.5 \text{ mm}$  and a depth of the notch of  $4.5 \text{ mm}$  was determined for the bending beam  $x'$  and a width of  $10 \text{ mm}$  and a depth of  $3 \text{ mm}$  for the bending beam  $y'$ . Figure 4 shows the results of the parameter study. The desired strain at the positions of the SG is almost achieved. That means that,  $950 \mu\text{m/m}$  are achieved for  $\text{SG } x'$  and  $910 \mu\text{m/m}$  for  $\text{SG } y'$ . Thus, the sensitivity is sufficient.

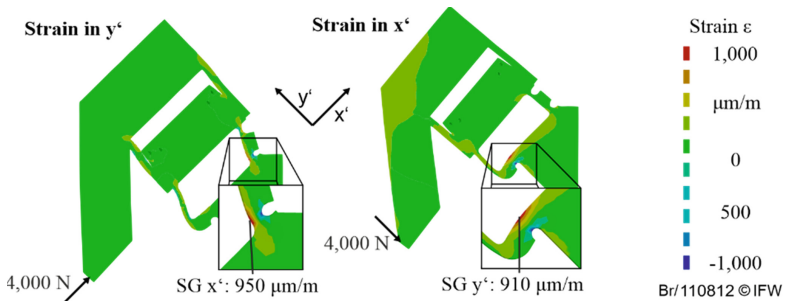


**Fig. 4.** Results of the Simulation

In order to be able to evaluate the position of the SG on the bending beams, the transfer matrix  $M$  was calculated using the simulation results. For this purpose, forces were applied in the machine coordinate system ( $x/z$ , Fig. 3) to the DRT. Then, the resulting mean strains at the location of the DMS were used to predict the voltage signal  $V_{x/y}$ . The  $k$ -factor of the SG, the amplification factor  $v_f$  of the electronics and the reference voltage  $U_{\text{ref}}$  of the Wheatstone bridge which were used for the calculation are shown in Fig. 5 on the left.  $M$  is a  $2 \times 2$  matrix. Thus, to calculate  $M$ , a  $2 \times 2$  matrix of  $F$  and  $V$  is needed. For this purpose, it is necessary to carry out the simulation for two direction of forces ( $F_1/F_2$ ). This results in the matrices  $F$  and  $V$  (Eq. 1). The transfer

matrix  $M$  is determined by solving (Eq. 2).

$$\begin{aligned}
 F &= [F_1 \ F_2] = \begin{bmatrix} F_{x,1} & F_{x,2} \\ F_{z,1} & F_{z,2} \end{bmatrix} \\
 &= M \cdot \begin{bmatrix} V_{x',1} & V_{x',2} \\ V_{y',1} & V_{y',2} \end{bmatrix} = M \cdot V \tag{1}
 \end{aligned}$$

$$\begin{aligned}
 M &= \begin{bmatrix} M_{1,1} & M_{2,1} \\ M_{1,2} & M_{2,2} \end{bmatrix} \\
 &= [M_1 \ M_2] = F \cdot V^{-1} \tag{2}
 \end{aligned}$$

Figure 5 (right) illustrates the vectors  $M_1$  and  $M_2$  of the matrix  $M$  graphically. It is obvious that the vectors are almost  $90^\circ$  to each other and  $M$  is thus well conditioned. Exactly  $90^\circ$  was not reached because the forces are never transmitted to just one bending beam, but both beams always experience a minimum load. According to [12], however, this confirms that the placement of the SG is favorable for a two-axis force measurement.

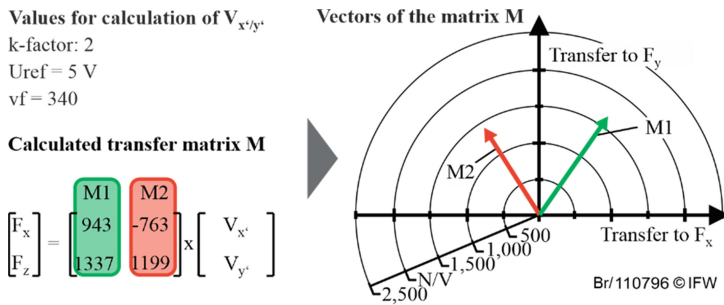


Fig. 5. Calculated transfer matrix from the results of the simulation

### 3 Calibration and Characterization of the Tool

The DRT was manufactured according to the design shown in Fig. 3 with the optimized parameters found through the simulation. To be able to determine the forces from the strain signals experimentally, the matrix  $M$  is needed. This Matrix was already calculated from the simulated results. However, for better accuracy, the matrix  $M$  was recalculated based on measured data. For the calculation, the SG signals for 11 different force directions were determined. Therefore, the setup in Fig. 6 was used. A Kistler 9129A multi-coordinate dynamometer supplies the reference force. An adapter with a radius of 15 mm was attached to the dynamometer to enable an application of forces in two dimensions. Forces in  $x$ - and  $z$ -direction were applied to the DRT while the forces and the SG signal were measured at the same time.

Figure 7 (left) shows the measured values of the SG signals  $V_{x'/y'}$  and the forces  $F_{x/z}$  which were used to calculate the matrix  $M$ . In contrast to the calculation according to

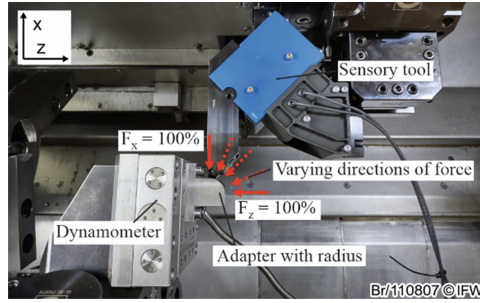


Fig. 6. Calibration of the tool

Eq. 2, the matrices  $V$  and  $F$  have the dimension  $2 \times n$  ( $n \gg 2$ ). The resulting system of equations is therefore overdetermined. The solution was determined using the least squares method according to Eq. 3.

$$M = F \cdot V^T \cdot (V \cdot V^T)^{-1} \tag{3}$$

The calculated matrix  $M$  is shown in Fig. 7 and is compared to the simulated matrix  $M$  (middle). When comparing the two transmission vectors  $M1/2$  graphically (right), a parallel alignment can be seen. However, the measured vectors are longer than the simulated ones. The length of the vector is inversely proportional to the sensitivity of the SG. Thus, a longer vector means that the sensitivity is lower. The sensitivity of the real DRT is reduced by a factor of 0.6 compared to the simulated DRT. This can be explained primarily by a reduced transmission of the strain to the SG in practice. In addition, imprecise placement of the SG can lead to deviations. However, the simulated nominal strain of about  $1000 \mu\text{m}/\text{m}$  is very high. A slight reduction in sensitivity is thus not a problem. Overall, however, this comparison shows that the tool corresponds to the simulated properties.

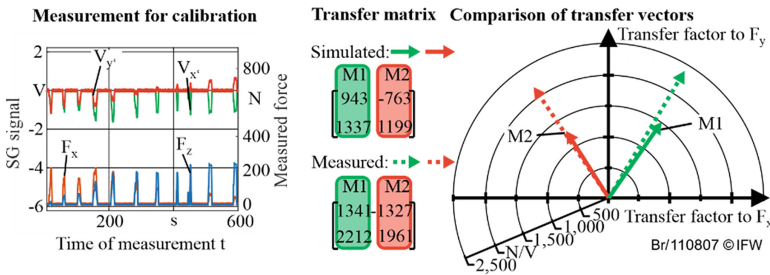


Fig. 7. Comparison of the simulated and measured transfer matrix

For a final evaluation of the force measurement capabilities, the force measured with the DRT was compared to that of the dynamometer. The force was varied from a load in x-direction to a load in z-direction as shown in Fig. 6. Thus, all possible load directions

are represented. To avoid overloading, the maximum force was limited to around 1 kN. Figure 8 shows the measured forces. On the left side, the whole measurement is shown for  $F_x$  and  $F_y$ . At the beginning, the measured Force was applied in x-direction. The cutout A (middle) shows the deviations occurring between the forces measured by the DRT and the dynamometer for a force in x-direction in more detail. It can be seen that a signal noise of about 20 N occurs. On the one hand, the noise comes from the SG itself, but electrical interference from the machine tool adds up. A systematic deviation of 15 N also occurs. This can be caused by an incorrect transmission matrix  $M$ . In addition, a non-linear behavior of the tool holder can lead to systematic deviations, because it is not taken into account by the transfer matrix. During the measurement the force was gradually varied from x-direction to z-direction. At the end of the measurement the force in z-direction was dominant. The cutout B shows the force in z-direction in more detail. The systematic deviation decreases to almost zero, but the signal noise is still about 20 N. Over all, a maximum total error of  $\pm 20$  N can be assumed. Based on the maximum force measured, this results in a relative error of 2%. Relative to the maximum load of 4000 N the error is 0.5%. Tests with existing tools had shown that a minimum resolution of  $\pm 100$  N is required for process monitoring of the deep rolling process. The force-sensitive DRT exceeds this resolution by factor five and is therefore suitable for process monitoring.

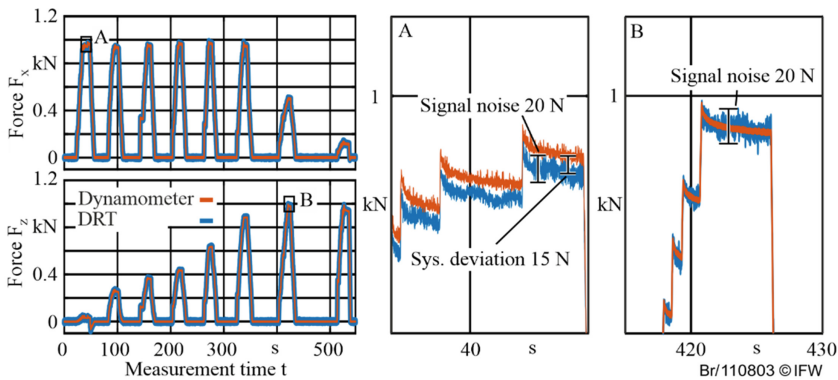


Fig. 8. Validation of the force measurement

## 4 Summary and Conclusion

The rolling force is a crucial variable for the deep rolling process. A force-sensitive rolling tool thus enables process monitoring. The development, commissioning and characterization of the tool was described in this paper. After introducing the basic concept for the tool, a simulation was used to optimize and evaluate it. Afterwards, the calibration process was described. Finally, experiments revealed that a force measurement with a maximum error of  $\pm 20$  N was achieved. In future works, the application of this tool for process monitoring is examined.

**Acknowledgements.** The cooperation project “Process-monitored and controlled mechanical deep rolling” (ZF4810001LP9/ZF4070523LP9) is funded by the Federal Ministry of Economics and Climate Protection (BMWK) as part of the Central Innovation Program for SMEs (ZIM) and is supervised by the Working Group of Industrial Research Associations (AiF). The ECOROLL AG thanks for the productive cooperation in this project. The MCU GmbH & Co. KG and the IFW thanks for the financial support.

## References

1. Delgado, P., Cuesta, I.-I., Alegre, J.-M., Díaz, A.: State of the art of deep rolling. *Precis. Eng.* **46**, 1–10 (2016)
2. Stichi, M., Schnubel, D., Kashaev, N., Huber, N.: Review of residual stress modification techniques for extending the fatigue life of metallic aircraft components. *Appl. Mech. Rev.* **67**(1), 010801(pp. 1–9) (2015)
3. Altenberger, I.: Deep rolling—the past, the present and the future. In: 9th International Conference on Shot Peening, pp. 144–155 (2005)
4. Milne, I., Ritchie, R.-O., Karihaloo, B.: *Comprehensive Structural Integrity: Cyclic Loading and Fatigue*. Elsevier Science Ltd. (2003)
5. Rodríguez, A., López de Lacalle, L.-N., Celaya, A., Lamikiz, A., Albizuri, J.: Surface improvement of Shafts by the deep ball-burnishing technique. *Surf. Coat. Technol.* **206**(11–12), 2817–2824 (2012)
6. Novovic, D., Dewes, R.-C., Aspinwall, D.-K., Voice, W., Bowen, P.: The effect of machined topography and integrity on fatigue life. *Int. J. Mach. Tools Manuf.* **44**(2–3), 125–134 (2003)
7. Manouchehrifar, A., Alasvand, K.: Finite element simulation of deep rolling and evaluate the influence of parameters on residual stress. In: 5th WSEAS, pp. 121–127 (2012)
8. Klocke, F., Mader, S.: Fundamentals of the deep rolling of compressor blades for turbo aircraft engines. *Steel Res. Int. Surf. Treat.* **76**(2–3), 229–235 (2005)
9. Denkena, B., Grove, T., Breidenstein, B., Abrão, A., Meyer, K.: Correlation between process load and deep rolling induced residual stress profile. In: 6th CIRP Global Web Conference, vol. 78, pp. 161–165 (2018)
10. Denkena, B., Litwinski, K.-M., Boujnah, H.: Process monitoring with a force sensitive axis-slide for machine tools. In: 2nd International Conference on System-Integrated Intelligence, vol. 15, pp. 416–423 (2014)
11. Boujnah, H., Denkena, B.: Kraftsensitiver Spindelschlitten zur online Detektion und Kompensation der Werkzeugabdrängung in der Fräsbearbeitung. *Tewiss, Hannover* (2019)
12. Litwinski, M., Denkena, B.: Sensorisches Spannsystem zur Überwachung von Zerspanprozessen in der Einzelteilmontage. *PZH GmbH, Hannover* (2011)
13. Maschinenmarkt.: Werkzeug-Spezialist Ecoroll treibt Entwicklung beim Glatt- und Festwalzen voran. <https://www.maschinenmarkt.vogel.de/werkzeug-spezialist-ecoroll-treibt-entwicklung-beim-glatt-und-fest-walzen-voran-a-93256/>. Last accessed 7 Apr 2022
14. Zhao, L., Zhao, Y.-L., Shao, Y.-W., Hu, T.-J., Zhang, Q., Ge, X.-H.: Research of a smart cutting tool based on MEMS strain gauge. *J. Phys. Conf. Ser.* **986**, 012016 (2018)